# Resonant Ring Fiber Filters

Liang Dong, George E. Berkey, Paul Chen, and David L. Weidman

***Abstract*—We have studied structures where a concentric ring with an index higher than that of the cladding index is added to a conventional fiber core. The structure supports at least one additional symmetric mode with substantial power in the ring, besides the normal mode in the core. Within certain designed parameter regime, the propagation constants of the lowest two symmetric modes cross at certain wavelength. This is equivalent to saying that LP01 mode can change from having more power in core to having more power in ring at certain wavelength or vice versa. At this resonance, each of the two modes has substantial power in the core and the ring. This resonant nature of the structure creates a strong wavelength dependent mode field for LP01 and LP02 modes near the resonance wavelength. Filters based on this principle are demonstrated for the first time.**

## I. Introduction

MISMATCHED twin-core fiber filters have been studies by various authors [1]–[3], and [4]. The design principle of the filters is to make the two core modes phase-matched at certain wavelength, so that coupling between the two cores can happen at this wavelength, while no coupling happen elsewhere in the wavelength spectrum. In addition to the high spectrum quality of the filters demonstrated [3], [4], there are a number of advantages of this type filters comparing to grating based filters. There are literally fibers, so they lend themselves to be mass-produced; filter wavelength can be adjusted over few hundred of nanometers from the same fiber; they are as reliable as fibers and they can be made truly distributive. Although mismatched twin core fiber filters can have low polarization dependence when coupling is weak, however polarization dependence can be a problem due to their intrinsic noncircular symmetry where stronger coupling or much longer device length is required.

Similar filters can also be implemented in fibers with an additional ring some distance away from the core. The outer ring and the central core play the parts of the two cores in the mismatched fiber filters case, when properly designed. The basic concept was touched upon by Cozens *et al.* in a theoretical paper in 1981 [5]. The same principle was also used by Boucouvalas *et al.*in their attempts to make tapered couplers [6]. The fiber will be referred as resonant ring fiber (RRF) in this paper. This configuration essentially solved the polarization dependence problem associated with mismatched twin-core fiber filters by having a circularly symmetric configuration and is especially appropriate for loss filters where no access to the optical power in the outer ring is required. This circular configuration also lends itself to be easily fabricated by vapor phase deposition techniques used for all fiber fabrication today. In this paper, we report the first experimental implementations of this type of filters.

Manuscript received January 20, 2000.

The authors are with Corning Incorporated, Corning, NY 14831 USA (e-mail: DongL@Corning.com).

Publisher Item Identifier S 0733-8724(00)05766-2.

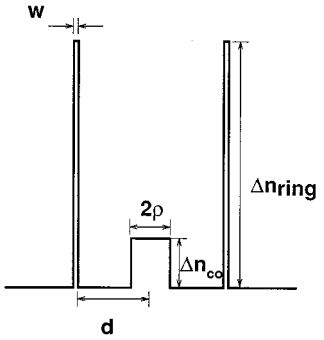


Fig. 1. Illustration of index profile of a resonant ring fiber.

In a mismatched twin core fiber consisting two adjacent cores with different designs, the fiber can support at least two modes with most power of each mode mainly concentrated over each core and the propagation constants of the two modes can be manipulated independently. Similarly in RRF, there can exist two symmetric modes with most power concentrated mainly over the core and ring respectively. The two modes will be referred as core mode and ring mode. The propagation constants of the core and ring modes can be manipulated independently to certain extent by varying the parameters of the core and ring respectively, and can therefore be designed to cross at certain wavelength, $\lambda_0$. This resonance at $\lambda_0$ is intrinsically the same as where the fundamental mode of the structure changes from one mode to another (ring mode to core mode or vice versa). At this resonance, strong periodic power transfer between core and ring can happen. An illustration of the index profile of a RRF is shown in Fig. 1, where a high index ring is added to a lower index fiber core. Definition of key parameters used in this paper is also shown. $\Delta n_{\rm co}$ is the core index difference; $\rho$ is core radius, $d$ is the distance from the center of the core to the edge of the ring; $\Delta n_{\rm ring}$ is the ring index difference; $W$ is the ring width. The LP01 and LP02 modes of the structure will be the coupling core and ring modes.

## II. Principle of Operation

Consider a structure with a thin high index ring and a large lower index core (the reverse will also work, i.e., a small higher index core and a wide low index ring), with appropriate design the fundamental mode of the structure can be the ring mode and the conventional core mode being LP02 mode. As the wavelength is increased, the propagation constant of the ring mode (LP01 at this wavelength) decreases much faster than the core mode (LP02 mode at this wavelength). At $\lambda_0$, a transition between the two modes happens and for $\lambda > \lambda_0$, the fundamental

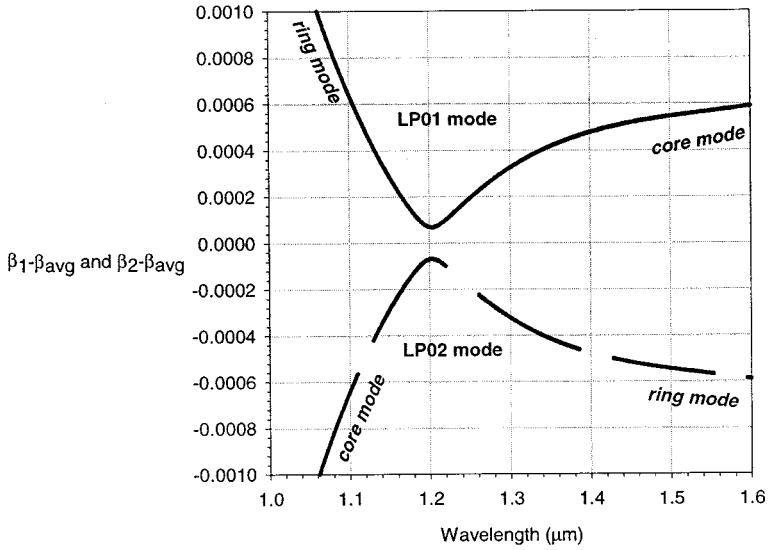


Fig. 2. Crossover of the propagation constants of the core and ring modes. Fiber parameters are: $\Delta n_{\rm co} = 0.0054$, $\rho = 3.83\ \mu$m, $d = 15\ \mu$m, $\Delta n_{\rm ring} = 0.025$ and $W = 0.53\ \mu$m. The fiber design gives $\lambda_0 = 1.205\ \mu$m.

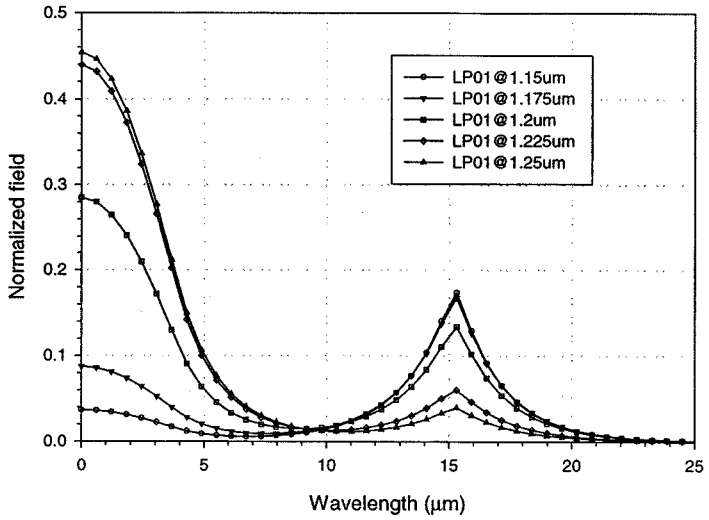


Fig. 3. LP01 modal fields at various wavelength around $\lambda_0 = 1.205\ \mu$m. Fiber parameters are the same as in Fig. 2.

mode (LP01 mode) becomes the core mode, which now has a higher propagation constant. Fig. 2 shows the behavior of the normalized propagation constants of the LP01 and LP02 modes during such a transition. Fiber parameters are: $\Delta n_{\rm co} = 0.0054$, $\rho = 3.83\ \mu$m, $d = 15\ \mu$m, $\Delta n_{\rm ring} = 0.025$ and $W = 0.53\ \mu$m. The fiber design gives $\lambda_0 = 1.205\ \mu$m. The LP01 mode's transition from ring mode to core mode at around $\lambda_0$ is also captured in Fig. 3, where the normalized modal fields of LP01 mode are plotted for five different wavelengths with a step of 25 nm. At $\lambda < \lambda_0$, the LP01 mode has most of its power in the ring while at $\lambda > \lambda_0$, LP01 mode has most of its power in the core. At $\lambda_0$, the LP01 and LP02 modes are plotted together in Fig. 4, showing that each mode has a substantial amount of power over the core and ring. In fact, the amplitude distribution of the fields is very similar both over the core and ring, with the LP01 mode maintaining a same phase whilst LP02 mode an opposite phase over the two regions. This is very similar to the two supper-modes in a mismatched twin core fiber. A corresponding strong waveguide dispersion is expected around $\lambda_0$ as a result of the transition. This is shown for LP01 mode in Fig. 5. Similarly to a typical resonant behavior, this dispersion peak can be increased with a reduction of bandwidth or vice versa.

In Fig. 6, a loss filter constructed from a RRF is illustrated. A section of the RRF is spliced between two conventional single mode fibers. At the entrance to the RRF, both the LP01 (even mode) and LP02 (odd mode) of the RRF are equally excited to satisfy the boundary condition that there is no power in the ring at the entrance to the RRF. The phase walk off between the two modes causes power to couple between the core and ring over a coupling length $L_c$. If RRF of $L_c$ long is used as in Fig. 6. There will be significant transmission loss at $\lambda_0$ and low transmission loss elsewhere as illustrated in Fig. 6.

In another configuration, ring can be made to have high loss to cause a continuous loss for light around $\lambda_0$, but not elsewhere.

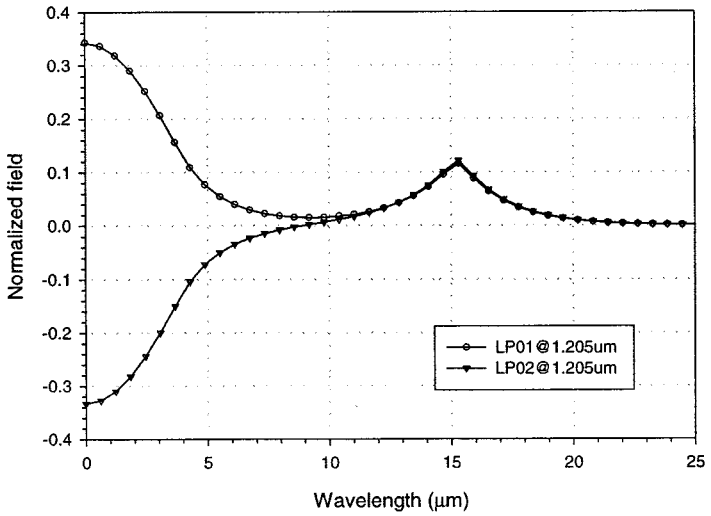


Fig. 4. LP01 and LP02 modes at $\lambda_0 = 1.205\ \mu$m. Fiber parameters are the same as in Fig. 2.

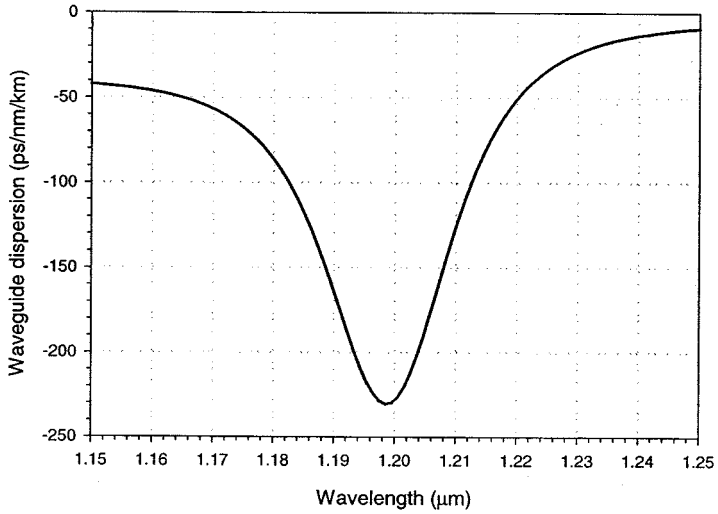


Fig. 5. LP01 mode waveguide dispersion around $\lambda_0 = 1.205\ \mu$m. Fiber parameters are the same as in Fig. 2.

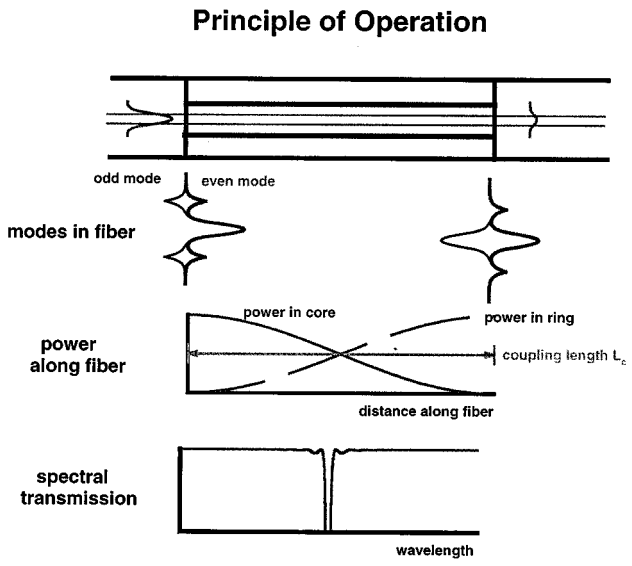


Fig. 6. Illustration of a loss filter constructed with a section of RRF.

Distributed spectral loss filter of tens of meters long can be made this way. The peak loss can be controlled by the amount of loss caused by the ring.

Tuning of RRF filter can be done similarly to what has been demonstrated in mismatched twin-core fiber filter [3]. The resonance peak can be changed by varying the fiber diameter with its relative internal structure unchanged [3]. This diameter change can be done on a fiber drawing tower by drawing the same preform into a fiber with a new desired diameter or using a set-up similar to that of a coupler rig to obtain a constant diameter reduction over a length of fiber [3]. The bandwidth of filters can be varied from few nanometers to over few tens of nanometers by suitable fiber designs.

## III. Experiments

### A. Filter Spectral Response

Several RRF's have been made with designs of both high index ring/low index core and high index core/low index ring.

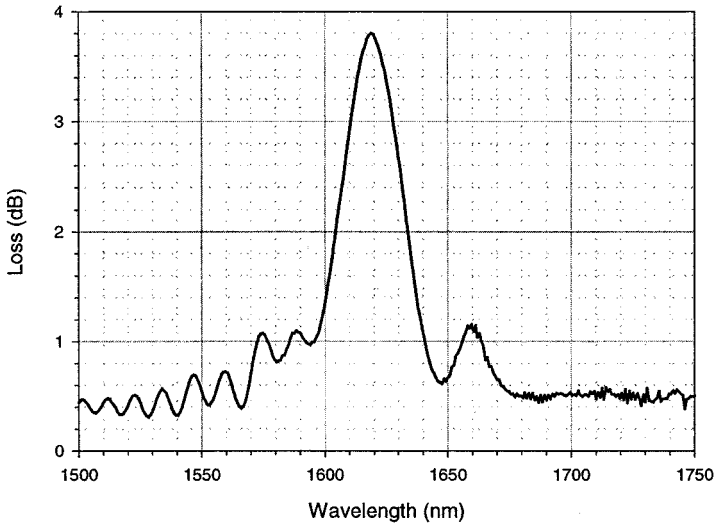


Fig. 7. Measured filter response with a section of RRF1 spliced between two SMF-28 fiber. Fiber parameters are $\Delta n_{co} = 0.0047$, $\rho = 4.85$ $\mu$m, $d = 16$ $\mu$m, $\Delta n_{\rm ring} = 0.0155$ and $W = 1.02$ $\mu$m. The length of RRF1 is 90 mm.

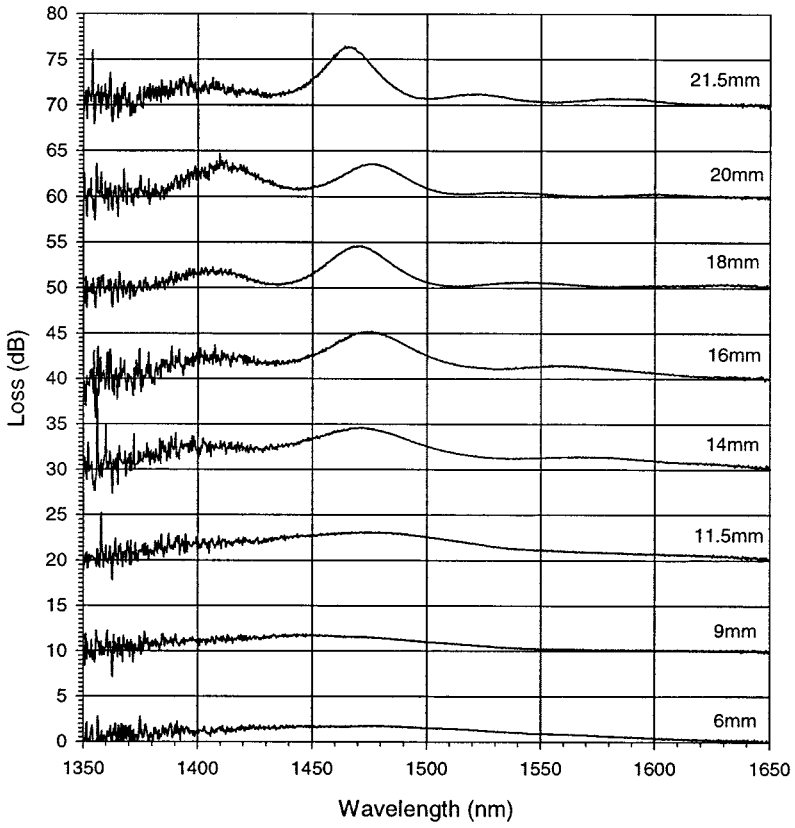


Fig. 8. Measured filter response with sections of RRF2 spliced between two SMF-28 fibers. RRF2 has a $\Delta n_{\rm co}$ of 0.0047, $\rho$ of 4.85 $\mu$m, $d$ of 14.2 $\mu$m, $\Delta n_{\rm ring}$ of 0.021 and $W$ of 0.82 $\mu$m., but with $\sim$4 wt% $B$ doped in the ring. The lengths of RRF2 are shown next to each curve.

Three fibers will be discussed in this paper. The first fiber has a $\Delta n_{\rm co}$ of 0.0047, $\rho$ of 4.85 $\mu$m, $d$ of 16 $\mu$m, $\Delta n_{\rm ring}$ of 0.0155 and $W$ of 1.02 $\mu$m. This fiber will be referred to as RRF1. From each preform, fibers with several different diameters were usually drawn. The second and third fibers both have a $\Delta n_{\rm co}$ of 0.0047, $\rho$ of 4.85 $\mu$m, $d$ of 14.2 $\mu$m, $\Delta n_{\rm ring}$ of 0.021 and $W$ of 0.82 $\mu$m. These fibers will be referred to as RRF2 and RRF3.

In addition to Ge doping, RRF2 and RRF3 have certain amount of $B$ doped in the ring. RRF2 and RRF3 have $B$ doping level of $\sim$4 wt% and $\sim$1 wt% respectively in the ring. Ge doping level in the ring is slightly adjusted to give a same index in the ring.

A filter constructed with 90 mm of RRF1 is shown in Fig. 7. The RRF1 is spliced between two SMF-28™ fiber as described i n Fig. 6. Fig. 7 shows the typical response expected of this type of filter. The FWHM bandwidth in this case is $\sim$25 nm. The high insertion loss of 0.5 dB is mainly splice loss. Response of filters constructed out of several different lengths of RRF2 is given in

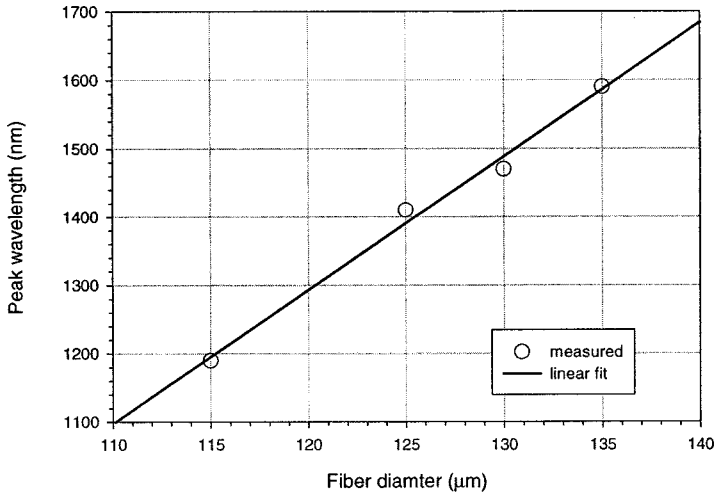


Fig. 9. Tuning curve of RRF2. The measured data (dots) is plotted together with the expected linear fit.

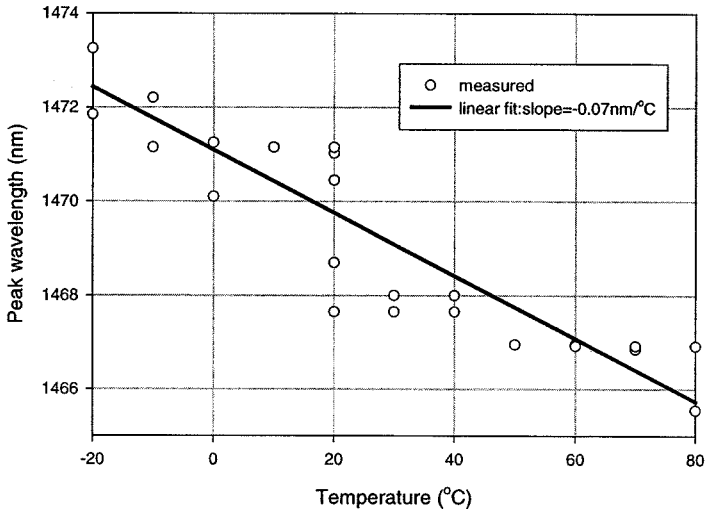


Fig. 10. Measured temperature sensitivity of the peak wavelength for RRF2 together with a linear fit with a slope of $-0.07$ nm/°C.

Fig. 8. The length of RRF2 used is given next to the each corresponding curves. Each curve is also displaced by 10 dB to show clearly all the curves. Fig. 8 shows the increase of peak loss as the length of RRF2 is increased from 6 mm to 21.5 mm. The narrowing of the filter as the RRF length increases is also expected from the theory and is consistent with this type of filters.

### *B. Filter Tuning Characteristics*

The filter center wavelength can be tuned by varying the fiber diameter, similarly as in mismatched twin-core filter. Fig. 9 gives the tuning curve for RRF2, together with a linear fit. The tuning curve is linear with a slope of 19.5 nm/$\mu$m. The peak wavelength is tuned over 400 nm as the fiber diameter varied from 115 to 135 $\mu$m.

### *C. Athermalization*

Athermalization of the filter can be achieved by equalizing the thermal dependence of the propagation constants of the two modes involved. If Ge doping is used to give the desired index profile, it will also give a higher thermal-optic coefficient to the ring in the design in Fig. 1. This will lead to higher thermal-optic coefficient to the ring mode. One way of achieving athermalization is by using appropriate codopants together with Ge doping to balance out the effect on the thermal dependence of the two propagation constants due to the different levels of Ge doping in core and ring of the fiber. One possible dopant is Boron. Since only a balance needs to be achieved so that only the part (core or ring depending design) with a high Ge content needs to be doped with an appropriate amount of $B$. RRF2 and RRF3 were made to check out the effect of $B$ doping in the ring of RRF1 on the thermal dependence of the RRF. Figs. 10 and 11 show the thermal response of RRF2 and RRF3, respectively. RRF2 and RRF3 have a temperature dependence of $-0.07$ and 0.09 nm/°C respectively, demonstrating the feasibility of tuning the temperature dependence by $B$ doping. $P$ can also be used to give a similar effect.

### *D. Tension Dependence of the Filter Wavelength*

A Filter constructed from RRF3 is measured when different amount of tension is applied for testing its dependence on tension. The measured peak wavelength is plotted at different ten-

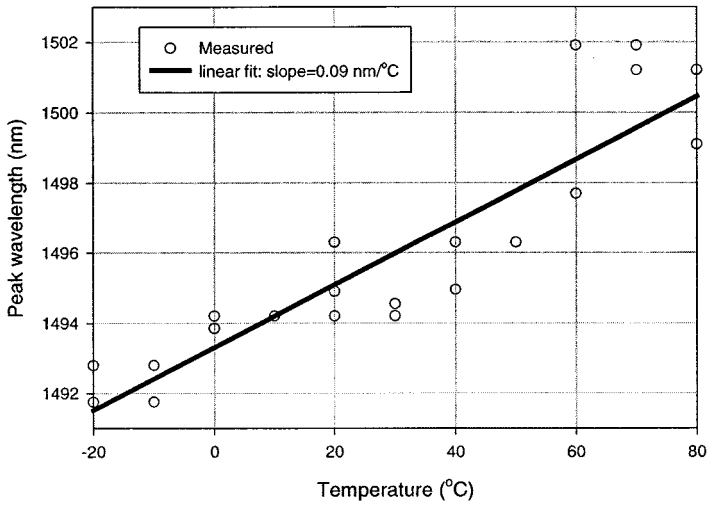


Fig. 11. Measured temperature sensitivity of the peak wavelength for RRF3 together with a linear fit with a slope of 0.09 nm/°C. RRF2 has a $\Delta n_{\rm co}$ of 0.0047, $\rho$ of 4.85 $\mu$m, $d$ of 14.2 $\mu$m, $\Delta n_{\rm ring}$ of 0.021 and $W$ of 0.82 $\mu$m., but with $\sim$1 wt% $B$ doped in the ring.

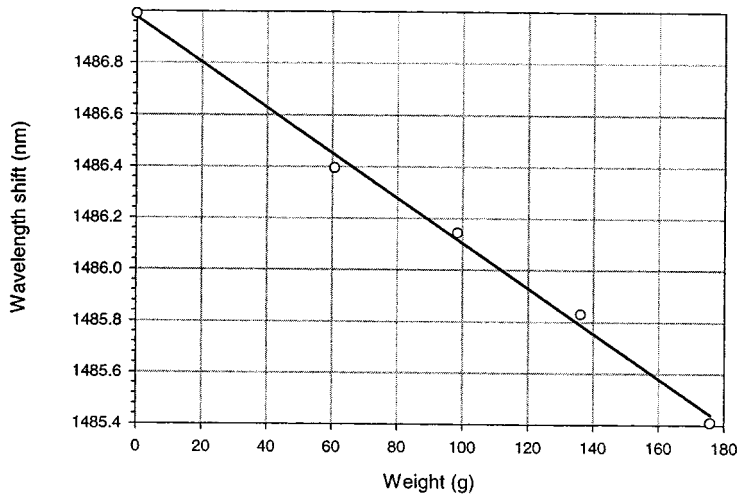


Fig. 12. Measured tension dependence for RRF3 together with a linear fit with a slope of $-8.7$ nm/Kg.

sion in grams in Fig. 12 together with a linear fit. The slope is $-8.7$ nm/kg.

## IV. Summary and Discussion

We have experimentally demonstrated a new type of spectral filters based entirely on fiber design. Such filter can be easily implemented to a strength of choice (up to more than 20 dB demonstrated) and wavelength of choice (over nearly 400 nm coverage demonstrated with one fiber). The filters are intrinsically more stable that filters based on interferometric technology.

Complex loss spectrum can also be implemented by cascading several filters of Fig. 6 in series, which each peak wavelength fine tuned by drawing the fiber to an appropriate diameter and peak loss finely tuned by choosing a right fiber length.

Athermalized filter can be achieved using $B$ or $P$ doping in the high Ge part of the fiber. Narrow band dispersion compensator and dispersion slope compensator are also possible using the high peak dispersion and high dispersion slope of the fiber.

## References

[1] G. Grasso, F. Fontana, A. Righetti, P. Scrivener, P. Turner, and P. Maton, "980 nm diode pumped Er-doped fiber optical amplifiers with high gain bandwidth product," in *Proc. Optic. Fiber Commun. Conf.*, Feb. 1991, p. 195.

[2] D. Marcuse, "Directional coupler filters using dissimilar optical fiber," *Electron. Lett.*, vol. 21, pp. 726–727, Sept. 1985.

[3] B. Ortega and L. Dong, "Accurate tuning of mismatched twin-core fiber filters," *Electron. Lett.*, vol. 23, pp. 1277–1279, Aug. 1998.

[4] ——, "Characteristics of mismatched twin-core fiber spectral filters," *IEEE Photon. Technol.Lett.*, vol. 10, pp. 991–993, July 1998.

[5] J. R. Cozens and A. C. Boucouvalas, "Coaxial optical coupler," *Electron. Letters.*, vol. 18, pp. 138–140, Feb. 1982.

[6] A. C. Boucouvalas and G. Georgiou, "Biconical taper coaxial optical fiber coupler," *Electron. Lett.*, vol. 21, pp. 864–864, Sept. 1985.

**Liang Dong**, photograph and biography not available at the time of publication.

**George E. Berkey**, photograph and biography not available at the time of publication.

**Paul Chen**, photograph and biography not available at the time of publication.

**David L. Weidman**, photograph and biography not available at the time of publication.